Journal of Systems Engineering and Electronics
Vol. 32, No. 4, August 2021, pp.831 – 840

Two-step compressed acquisition method for Doppler frequency and Doppler rate estimation in high-dynamic and weak signal environments

WU Chao[1,2,*], LIU Erxiao[1], and JIAN Zhihua[1]

1. School of Communication Engineering, Hangzhou Dianzi University, Hangzhou 310018, China;
2. School of Electronics and Information, Northwestern Polytechnical University, Xi'an 710082, China

Abstract: To acquire global navigation satellite system (GNSS) signals means four-dimension acquisition of bit transition, Doppler frequency, Doppler rate, and code phase in high-dynamic and weak signal environments, which needs a high computational cost. To reduce the computations, this paper proposes a two-step compressed acquisition method (TCAM) for the post-correlation signal parameters estimation. Compared with the fast Fourier transform (FFT) based methods, TCAM uses fewer frequency search points. In this way, the proposed method reduces complex multiplications, and uses real multiplications instead of improving the accuracy of the Doppler frequency and the Doppler rate. Furthermore, the differential process between two adjacent milliseconds is used for avoiding the impact of bit transition and the Doppler frequency on the integration peak. The results demonstrate that due to the reduction of complex multiplications, the computational cost of TCAM is lower than that of the FFT based method under the same signal to noise ratio (SNR).

Keywords: high-dynamic and weak signal environment, compressed acquisition, frequency parameters estimation.

DOI: 10.23919/JSEE.2021.000072

1. Introduction

Global navigation satellite system (GNSS) signal acquisition plays a very important role in the software defined receiver (SDR), and Doppler frequency and code phase should be estimated in this stage for location-based services (LBSs). In the GNSS-challenged environments [1−3], a fast acquisition method with low computational complexity [4−7] is needed. Furthermore, with integration time increasing, the acquisition may need four-dimension detection of bit transition, Doppler frequency, Doppler rate, and code phase.

Compared with the fast Fourier transform (FFT)-based method [8], the method in [9] compressed code phases to realize the fast acquisition. To further reduce the computational complexity, the Doppler frequency and code phase two-dimension compress method [10] has been proposed. However, those methods [9,10] ignore the effect of bit transition on the integration peak. To solve the problem, Zhu et al. [11] proposed the weak acquisition method extending the coherent integration time to one entire navigation data bit duration based on FFT. To reduce the computational burden, Kong et al. [12] proposed the synthesized Doppler frequency hypothesis testing (SDHT) method, which reduced the number of Doppler frequency searches. However, the impact of the Doppler rate on integration is not considered in the SDHT, which is an important factor for integration peak detection in high-dynamic acquisition [13−15].

For acquisition in the high-dynamic and weak signal environments [16,17], four-dimension detection of bit transition [18,19], Doppler frequency[20], Doppler rate, and code phase is needed [21], which costs more computational burdens compared with the two-dimension acquisition. Frequency parameters estimation includes Doppler frequency and Doppler rate estimation. Due to the reason that frequency parameters interact with each other, the differential process [22−25] can be used. To reduce the computational burden in the high-dynamic and weak signal environments, Yang et al. [21] proposed a block accumulating semi-coherent integration of the correlations method (BASIC). Regardless of bit sign transition, Luo et al. [26] proposed the post-correlation signal parameters estimation method based on the fractional Fourier transform (FRFT) for high-dynamic signals. The probability of bit transition is analyzed for improving the detec-

Manuscript received June 09, 2020.
*Corresponding author.
This work was supported by the National Natural Science Foundation of China (61901154; 41704154), and Zhejiang Province Science Foundation for Youths (LQ19F010006).

tion probability in [27]. Since discrete chirp-Fourier transform (DCFT) can be used to improve the L5 signal acquisition detection probability [28], we proposed a block zero-padding method based on DCFT for parameter estimation in weak signals and high dynamic environments in [29]. In this way, the post-correlation signal is coherently post-integrated with the bit sequence stripped off, and the high dynamic parameters are precisely estimated using the threshold set based on a false alarm probability [30,31]. However, DCFT costs a lot of computations, the detection efficiency needs to be further improved.

To further reduce the computational complexity in high-dynamic and weak signal environments, the two-step compressed acquisition method (TCAM) has been proposed in this paper. In the simulated test, because mean acquisition computation (MAC) contains the effect of detection performance and computational complexity on the acquisition method, MAC is chosen as the assessment criteria of acquisition efficiency. Since TCAM has compressed the number of frequency parameters search and reduced complex multiplications, the computational cost of TCAM is lower than that of the FFT based method under the same signal to noise ratio (SNR).

This paper is organized as follows. Firstly, the high-dynamic post-correlation signal model is derived. Then, to avoid effect of bit sign, Doppler frequency and Doppler rate on the detection peak, the differential process is depicted. Moreover, TCAM for Doppler frequency and Doppler rate estimation have been proposed. The detection probabilities and MAC of TCAM are derived and analyzed. Finally, the tests for acquisition performance comparison are proposed.

2. Signal model

In the absence of noise, the received intermediate frequency (IF) signal can be modeled as

$$r_I(n_t)=AC_\tau(n_t)B(n_t)\cdot \exp\left[\mathrm{j}2\pi\left((f_I+f_d)n_tT_t+\alpha_0n_t^2T_t^2\right)+\mathrm{j}\varsigma_0\right] \tag{1}$$

where A represents the amplitude of the IF signal, $C_\tau(\cdot)$ represents the pseudorandom code with initial code phase τ, $B(\cdot)$ represents the bit sign, f_I represents IF, f_d represents the Doppler frequency, α_0 represents the Doppler rate, T_t represents the sampling interval of digital IF, and ς_0 represents the initial phase. The local code can be constructed as

$$L_I(n_t)=C(n_t)\exp\left[-\mathrm{j}2\pi\left(f_I+f_{k_f}\right)n_tT_t\right] \tag{2}$$

where $f_{k_f}=2k_fM_f\Delta_f$, where $\Delta_f=1/(2T)$ with T being the integration time (IT) and M_f represents the compression factor of the Doppler frequency, $k_f=-K_f,-K_f+1,\cdots,K_f$ represents the search index. Considering the code phase and the Doppler frequency, the post-correlation signal $R(n)$ can be expressed as

$$\begin{aligned}R(n)&=\frac{1}{N_t}\sum_{n_t=nN_t}^{(n+1)N_t-1}r_I(n_t)L_I(n_t)\approx\\&\frac{A}{N_t}B(n)\sum_{n_t=nN_t}^{(n+1)N_t-1}C(n_t)C_\tau(n_t)\cdot\\&\sum_{n_t=nN_c}^{(n+1)N_t-1}\exp\left[\mathrm{j}2\pi\left(\left(f_d-f_{k_f}\right)n_tT_t+\alpha_0n_t^2T_t^2\right)+\mathrm{j}\varsigma_0\right]\approx\\&\frac{A}{N_t}B(n)\sum_{n_t=nN_t}^{(n+1)N_c-1}C(n_t)C_\tau(n_t)\cdot\\&\sum_{n_t=nN_t}^{(n+1)N_t-1}\exp\left[\mathrm{j}2\pi\bar{f}n_tT_t+\mathrm{j}\varsigma_0\right]\end{aligned} \tag{3}$$

where N_t represents the number of samples per code period, $\bar{f}$ represents the average frequency between intervals nN_tT_t and $((n+1)N_t-1)T_t$, and is equal to $f_0+\alpha_0nN_tT_t+\alpha_0\frac{N_t-1}{2}T_t$, where $f_0=f_d-f_{k_f}$. When the local code is aligned with the received signal, (3) can be simplified to

$$\begin{aligned}R(n)&\approx AB(n)\left(1-\frac{|i_cT_t-\tau|}{T_c}\right)\frac{1-\exp\left(\mathrm{j}2\pi\bar{f}T_s\right)}{1-\exp\left(\mathrm{j}2\pi\bar{f}T_t\right)}\cdot\\&\exp\left[\mathrm{j}2\pi\bar{f}nT_s+\mathrm{j}\varsigma_0\right]=\\&B(n)A\left(1-\frac{|i_cT_t-\tau|}{T_c}\right)\frac{\sin\left(\pi\bar{f}T_s\right)}{\sin\left(\pi\bar{f}T_t\right)}\cdot\\&\exp\left[\mathrm{j}\pi\bar{f}(2n+1)T_s-\mathrm{j}\pi\bar{f}T_t+\mathrm{j}\varsigma_0\right]\end{aligned} \tag{4}$$

where $\left|i_cT_f-\tau\right|\leqslant T_c$, T_c is the chip duration, $T_s=N_tT_t$. Since $\pi\bar{f}T_t$ is really small,

$$R(n)\approx A_{f_{k_f},n,i_c}B(n)\exp\left[\mathrm{j}\pi\bar{f}(2n+1)T_s+\mathrm{j}\varsigma_0\right] \tag{5}$$

where $A_{f_{k_f},n,i_c}=AN_c\left(1-\frac{|i_cT_t-\tau|}{T_c}\right)\mathrm{sinc}\left(\pi\bar{f}T_s\right)$, $n=0,1,\cdots,N_s$, $T=N_sT_s$.

3. Proposed method

In this section, to estimate the frequency parameters (f_0 and α) efficiently, the two compressed processes have been stated for avoiding the interaction among bit sign, Doppler frequency and Doppler rate respectively. Then, the parameters estimation method based on combining the two processes has been proposed.

3.1 Compressed Doppler rate estimation process

The differential process [25] can be performed, and the differential signal $d(n_d)$ can be written as

$$d_{b_0}(n_d)=R^*(n_d)R(n_d+N_B)=$$
$$A_{f_{k_f},n_d,i_c}A_{f_{k_f},n_d+N_B,i_c}B(n_d)B(n_d+N_B)\cdot\exp\left(\mathrm{j}2\pi\bar{f}T_s\right)=$$
$$A_\alpha B(n_d)B(n_d+N_B)\exp\left[\mathrm{j}4\pi n_d N_B\alpha_0 T_s^2+\mathrm{j}\varphi_0\right] \quad (6)$$

where n_d=b_0, $b_0+1,\cdots$, $N_s-N_B+b_0-1$, b_0=0,$\cdots$, N_B−1, and N_B represents the number of samples per bit period, φ_0=j$\pi N_s T_s[2f_0+\alpha_0(N_t-1)T_t+\alpha_0(N_B+1)T_s]$, $A_\alpha=A_{f_{k_f},n_d,i}d_{f_{k_f},n_d+N_B,i}$.

Now α_0 can be solved by Doppler rate search. Assuming that $L_\alpha(n_d,\alpha_k)$ is the local signal, it can be written as

$$L_\alpha(n_d,\alpha_{k_\alpha})=\exp\left(-\mathrm{j}4\pi n_d\alpha_{k_\alpha}N_BT_s^2\right) \quad (7)$$

where α_{k_α}=$2k_\alpha M_\alpha\Delta_\alpha$, $k_\alpha=-K_\alpha,\cdots,K_\alpha-1,K_\alpha$ represents the search index, M_α represents the compression factor of the Doppler rate, and Δ_α is the estimation accuracy of the Doppler rate.

Suppose

$$\varphi_{b_0}(n_d,\Gamma_1)=d_{b_0}(n_d)L_\alpha(n_d,\alpha_{k_\alpha}) \quad (8)$$

and

$$\varphi_{b_0}(n_1,\Gamma_1)=\sum_{n_d=(n_1-1)N_B+1}^{n_1N_B}\varphi_{b_0}(n_d,\Gamma_1) \quad (9)$$

where n_1=1,$\cdots$, N_{SB}, $N_{SB}=N_s/N_B-1$, and $\Gamma_1=k_\alpha$. For detecting the bit transition position, it is assumed that $\varphi(d,b_0)$ can be written as

$$\varphi(k,b_0)=\left(\begin{array}{ccc}\varphi_{b_0}(1,k_\alpha) & \cdots & \varphi_{b_0}(N_{SB},k_\alpha)\end{array}\right)\boldsymbol{D} \quad (10)$$

where $\boldsymbol{D}=[\boldsymbol{D}_k],k=1,\cdots,2^{N_{SB}-1},D_k=[b_1,\cdots,b_g,\cdots,b_{N_{SB}}]^{\mathrm{T}}$, and $b_g\in\{1,-1\}$. The detection variable J_1 for Doppler rate estimation detection can be written as

$$J_1=\max_{k,b_0}|\varphi(k,b_0)|^2. \quad (11)$$

When α_{k_α}=$2k_\alpha M_\alpha\Delta_\alpha$ and $J_1\geqslant T1$ ($T1$ means a threshold value), the estimated Doppler rate is α_{k_α}. If $J_1<T1$, the search accuracy of the Doppler rate should be improved by the following process:

$$\varphi_{b_0}\left(n_d,k_\alpha+\frac{g_1}{2^{h_1-1}}\right)+\varphi_{b_0}\left(n_d,k_\alpha+\frac{g_1+1}{2^{h_1-1}}\right)=$$
$$2\varphi_{b_0}\left(n_d,k_\alpha+\frac{g_1+0.5}{2^{h_1-1}}\right)\cos\left(\pi n_d\frac{N_BM_\alpha\Delta_\alpha}{2^{h_1-3}}T_s^2\right) \quad (12)$$

where $h_1=1,2,\cdots,\lceil 1+\log_2M_\alpha\rceil$, $g_1=1,2,\cdots,2^{h_1-1}$. $4\pi N_sM_\alpha N_B\Delta_\alpha T_s^2<\frac{\pi}{2}$. Based on (12), $\varphi_{b_0}\left(n_d,k_\alpha+\frac{g_1+0.5}{2^{h_1-1}}\right)$ can be obtained, and $\varphi_{b_0}(n_d,\Gamma_1)$ in (9) is updated. Then, the detection process based on (9) to (11) should be repeated. Based on (12), only complex additions and real multiplications are needed compared with complex multiplications used by (8), and Doppler rate accuracy can be improved. Moreover, $\varphi_1\left(n_d,k_\alpha+\frac{g_1}{2^{h_1-1}}\right)$ and $\varphi_1\left(n_d,k_\alpha+\frac{g_1+1}{2^{h_1-1}}\right)$ can be obtained from memory, and $\cos\left(\pi n_d\frac{M_\alpha\Delta_\alpha}{2^{h_1-3}}T_s^2\right)$ can be calculated in advance, which will not cost computation in acquisition process.

3.2 Compressed Doppler frequency estimation process

The parameter α_0 and bit transition of signal $R(n)$ can be estimated by Doppler rate search. Then, the signal $\varphi_2(n,k_f)$ for the compressed frequency estimation process can be modeled as

$$\varphi_2(n,k_f)\approx A_{f_{k_f},n,i}\exp[\mathrm{j}\pi f_0(2n+1)T_s+\mathrm{j}\varsigma_0]. \quad (13)$$

Based on the integration process, detection variable J_2 for Doppler frequency estimation corresponding to i_0 can be written as

$$J_2=\left|\sum_{n=0}^{N_s-1}\varphi_2(n,k_f)\right|^2. \quad (14)$$

When f_{k_f}=$2k_fM_f\Delta_f$ and $J_2\geqslant T2$, the estimated Doppler frequency is f_{k_f}. If $J_2<T2$, the search accuracy of Doppler frequency should be improved by the following process:

$$\varphi_2\left(n,k_f+\frac{g_2}{2^{h_2-1}}\right)+\varphi_2\left(n,k_f+\frac{g_2+1}{2^{h_2-1}}\right)=$$
$$2\varphi_2\left(n,k_f+\frac{g_2+0.5}{2^{h-1}}\right)\cos\left(\frac{M_f\Delta_f\pi(2n+1)T_s}{2^{h_2-1}}\right) \quad (15)$$

where $h_2=1,2,\cdots,\lceil 1+\log_2M_f\rceil$, $g_2=1,2,\cdots,2^{h_2-1}$. Based on the analysis [21,12], when $M_f=\frac{N_s}{2}$, $\Delta_f=\frac{1}{2T}=\frac{1}{2N_sT_s}$, $A_{f_{k_1},n,i1}\approx A_{f_{k_2},n,i2}\approx A_{f_{k_3},n,i3}$, $k_1=k_f+\frac{g_2}{2^{h_2-1}}$, $k_2=k_f+\frac{g_2+0.5}{2^{h_2-1}}$, and $k_3=k_f+\frac{g_2+1}{2^{h_2-1}}$. Equation (15) can be simplified as

$$\varphi_2\left(n,k_f+\frac{g_2}{2^{h_2-1}}\right)+\varphi_2\left(n,k_f+\frac{g_2+1}{2^{h_2-1}}\right)=$$
$$2\varphi_2\left(n,k_f+\frac{g_2+0.5}{2^{h_2-1}}\right)\cos\left(\frac{\pi(2n+1)}{2^{h_2+1}}\right). \quad (16)$$

Then, the detection process based on (14) should be repeated until $J_2\geqslant T2$. Based on (16), only real additions and real multiplications are needed compared with complex multiplications used by (3), and Doppler frequency accuracy can be improved. Moreover, $\varphi_2\left(n,k_f+\frac{g_2}{2^{h_2-1}}\right)$ and $\varphi_2\left(n,k_f+\frac{g_2+1}{2^{h_2-1}}\right)$ can be obtained from memory, and $\cos\left(\frac{\pi(2n+1)}{2^{h_2+1}}\right)$ can be calculated in advance, which will

not cost computation in the acquisition process. Moreover, $\cos\left(\frac{\pi(2n+1)}{2^{h_2+1}}\right)$ is the periodic function with the period 2^{h_2+1}. Thus J_2 for Doppler frequency estimation corresponding to $k_f+\frac{g_2+0.5}{2^{h_2-1}}$ can be written as

$$J_2=\left|\sum_{n=0}^{N_s-1}\varphi_2\left(n,k_f+\frac{g_2+0.5}{2^{h_2-1}}\right)\right|^2=\left|\sum_{i_n=0}^{2^{h_2+1}}\frac{\sum_{n_h=1}^{N_h}\varphi_2\left(i_n+2^{h_2+1}n_h,k_f+\frac{g_2}{2^{h_2-1}}\right)+\varphi_2\left(i_n+2^{h_2+1}n_h,k_f+\frac{g_2+1}{2^{h_2-1}}\right)}{\cos\left(\frac{\pi(2i_n+1)}{2^{h_2+1}}\right)}\right|^2 \tag{17}$$

where $2^{h_2+1}N_h$ is the smallest integer that is bigger than N_s.

3.3 TCAM for Doppler frequency and Doppler rate estimation

The TCAM has been shown in Fig. 1, and can be depicted with more details as follows.

Step 1 In the presence of noise, the received post-correlation signal $R_s(n)$ can be modeled as

$$R_s(n)=R(n)+w(n) \tag{18}$$

where both the real part and the imaginary part of $w(n)$ obey a normal distribution with mean value 0 and variance σ^2. Then, same as the process of (6), the differential signal $d_{b_0}(n_d)$ can be obtained, and $\varphi_{b_0}(n_d,\Gamma_1)$ can be obtained based on (8), where $\Gamma_1=k_\alpha$. Furthermore, based on (9) to (11), the integration process can be performed, and the detection variable J_1 for Doppler rate estimation detection can be obtained. If J_1 is bigger than the set threshold $T1$, the bit transition positon d_s and estimated Doppler rate $\overline{\alpha}$ can be obtained. Otherwise, $h_1=h_1+1$, and the improvement of search accuracy of the Doppler rate should be performed based on (12). In Fig. 1, $\varphi_1(h_1,g_1)$, $\varphi_1(h_1,g_1+0.5)$, and $\varphi_1(h_1,g_1+1)$ represent $\varphi_{b_0}\left(n_d,k_\alpha+\frac{g_1}{2^{h_1-1}}\right)$, $\varphi_{b_0}\left(n_d,k_\alpha+\frac{g_1+0.5}{2^{h_1-1}}\right)$ and $\varphi_{b_0}\left(n_d,k_\alpha+\frac{g_1+1}{2^{h_1-1}}\right)$ in the presence of noise, respectively. If $h_1>\lceil 1+\log_2 M_\alpha\rceil$ and $J_1<T_1$, it proves that the signal is absent, or the acquisition fails.

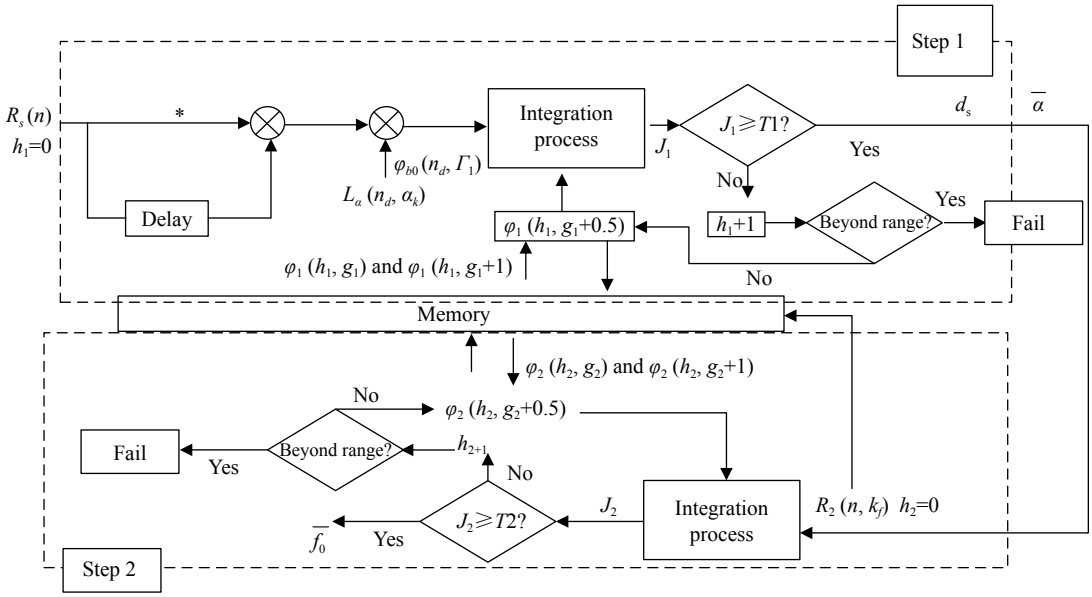

Fig. 1 TCAM diagram

Step 2 If the bit transition positon d_s and the estimated Doppler rate $\overline{\alpha}$ can be obtained from Step 1, Step 2 should be performed. Based on d_s and $\overline{\alpha}$, $R_2(n,k_f)$ can be obtained after processing $R_s(n)$:

$$R_2(n,k_f)\approx\varphi_2(n,k_f)+w(n). \tag{19}$$

Based on (14), the integration process can be performed, and the detection variable J_2 for Doppler frequency estimation detection can be obtained. If J_2 is bigger than the set threshold $T2$, the estimated Doppler frequency $\overline{f}_0$ can be obtained. Otherwise, $h_2=h_2+1$, and the improvement of search accuracy of the Doppler frequency should

be performed based on (16). In Fig. 1, $\varphi_2(h_2,g_2)$, $\varphi_2(h_2, g_2+0.5)$, and $\varphi_2(h_2,g_2+1)$ represent $\varphi_2\left(n,k_f+\frac{g_2}{2^{h_2-1}}\right)$, $\varphi_2\left(n,k_f+\frac{g_2+0.5}{2^{h_2-1}}\right)$, and $\varphi_2\left(n,k_f+\frac{g_2+1}{2^{h_2-1}}\right)$ in the presence of noise, respectively. Then, based on (17), the integration process can be performed and J_2 can be obtained. If $h_2>\lceil 1+\log_2 M_f\rceil$ and $J_2<T2$, it proves that the signal is absent, or acquisition fails.

4. Performance analysis

Based on the analysis in [24], it is hard to accomplish the statistical characterization of the detection variables, and the Gaussian distribution is used to approximate this probability distribution. Based on (11) and (14), the detection variables can be written as

$$J_i=\left|\sum_{n=0}^{N-1}(x_{i,n}+\mathrm{j}y_{i,n})\right|^2=\left(\sum_{n=0}^{N-1}x_{i,n}\right)^2+\left(\sum_{n=0}^{N-1}y_{i,n}\right)^2 \tag{20}$$

where $i=1,2$. $x_{i,n}$ and $y_{i,n}$ are real numbers. The central limit theorem states that if a sufficient number of summed random variables have a finite variance then the sum will be approximately normally distributed [22]. Based on the theory, $\sum_{n=0}^{N-1}x_{i,n}\sim \mathrm{N}\left(\mu_{x,i},\sigma_{x,i}^2\right)$, and $\sum_{n=0}^{N-1}y_{i,n}\sim \mathrm{N}\left(\mu_{y,i},\sigma_{y,i}^2\right)$, where $\mathrm{E}\left(\sum_{n=0}^{N-1}x_{i,n}\right)=\mu_{x,i}$, $\mathrm{E}\left(\sum_{n=0}^{N-1}y_{i,n}\right)=\mu_{y,i}$, $\mathrm{D}\left(\sum_{n=0}^{N-1}x_{i,n}\right)=\sigma_{x,i}^2$, and $\mathrm{D}\left(\sum_{n=0}^{N-1}y_{i,n}\right)=\sigma_{y,i}^2$. $\mathrm{E}(\cdot)$, $\mathrm{D}(\cdot)$, and $\mathrm{N}(\cdot)$ represents expectation operation, variance operation, and normal distribution, respectively.

Based on the analysis above, J_i obeys non-central chi-square distribution 2 m degrees of freedom [32], the probability density function (PDF) of J_i can be written as

$$p(J_i)=\frac{1}{2\sigma_i^2}\left(\frac{J_i}{a_i^2}\right)^{(m-1)/2}\exp\left(-\frac{J_i+a_i^2}{2\sigma_i^2}\right)\mathrm{I}_{m-1}\left(\sqrt{\frac{a_i^2J_i}{\sigma_i^4}}\right) \tag{21}$$

where $\mathrm{I}_m(\cdot)$ represents the m-order modified Bessel function with first kind. m=1. $a_i^2=(\mu_{x,i})^2+(\mu_{y,i})^2$. $\sigma_i^2=\sigma_{y,i}^2=\sigma_{x,i}^2$. Suppose H_1 represents the right detected cell, and H_0 represents the wrong detected cell, then the detection probability under different conditions can be written as

$$P\{J_i\geqslant T|H_0\quad\text{or}\quad H_1\}=Q_m\left(\frac{a}{\sigma},\frac{\sqrt{T}}{\sigma}\right) \tag{22}$$

where

$$Q_m(\gamma,\beta)=\frac{1}{\gamma^{m-1}}\int_\beta^{+\infty}x^m\exp\left(-\frac{x^2+\gamma^2}{2}\right)\mathrm{I}_m(\gamma x)\,\mathrm{d}x. \tag{23}$$

When the wrong detection unit is detected, the false alarm probability of J_i $P_{i,fa}=P\{J_i\geqslant Ti|H_0\}$. In Step i, Ti is set based on $P_{i,FA}$ belonging to $P_{i,fa}$ and corresponding to $a_{i,\max}^2$ which is the maximum of a_i^2. When the right detection unit is detected, $P_{1,D}=P\{J_1\geqslant T1|H_1\}$ represents the detection probability of the Doppler rate, and $P_{2,D}=P\{J_2\geqslant T2|H_1\}$ represents the detection probability of Doppler frequency. The miss detection probability $P_{i,M}=1-P_{i,D}$. The value of $P_{1,D}P_{2,D}$ is equal to the detection probability of the Doppler rate and the Doppler frequency.

In Fig. 2, T represents theoretical detection probabilities and S represents simulated detection probabilities, when post-correlation signal length is 60 ms or 80 ms. Since $4\pi N_sM_\alpha N_B\Delta_\alpha T_s^2<\frac{\pi}{2}$, it is assumed that $M_\alpha\Delta_\alpha=1/(8N_sN_BT_s^2)$ in the following discussion. When M_α increases, multiplications in TCAM can be reduced based on (8) and (12). However, the detection probability of the Doppler rate when M_α=3 is lower than that when M_α=2 in Fig. 2 (a). Thus M_α=2 is chosen in the following analysis. The false alarm probability $P_{1,FA}$=0.002, the number of Monte-Carlo is 10 000, f_0=Δ_f/3 Hz, and α_0=Δ_α/3 Hz/s.

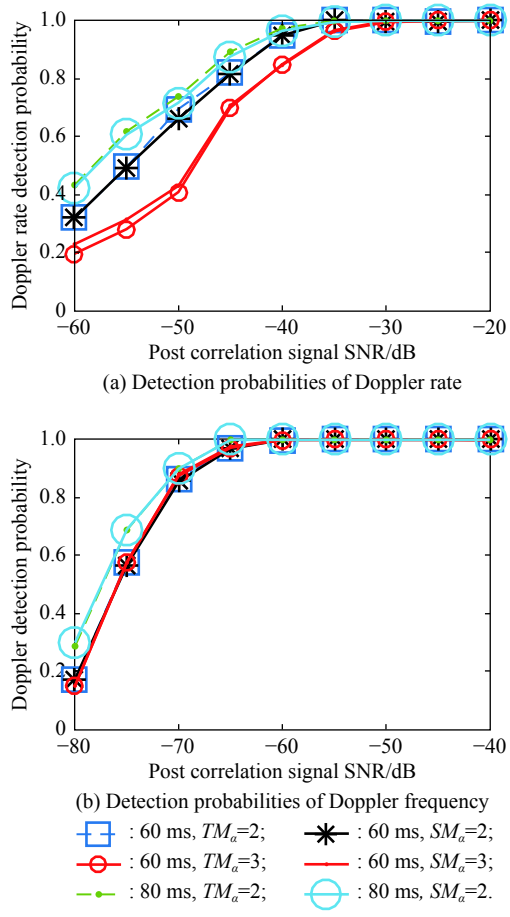

(a) Detection probabilities of Doppler rate

(b) Detection probabilities of Doppler frequency

Fig. 2 TCAM detection probabilities

In the search state diagram, M_1 represents the number of search for the Doppler rate, and M_2 represents the

number of search for the Doppler frequency. Based on Fig. 3 and the analysis in [12], the overall transfer function for the computational complexity can be found as

$$G(c) = G_1(c)G_2(c) \tag{24}$$

where

$$G_i(c) = \frac{G_{i,D}(c)\left[1 - G_{i,F}^{M_i}(c)\right]}{M_i\left[1 - G_{i,F}(c)\right]\left[1 - G_{i,M}(G_{i,F}(c))^{M_i - 1}\right]}, \tag{25}$$

$$G_{i,D}(c) = P_{i,D}c^{N_{c,i}}, \tag{26}$$

$$G_{i,M}(c) = P_{i,M}c^{N_{c,i}}, \tag{27}$$

$$G_{i,F}(c) = (1 - P_{i,FA})c^{N_{c,i}}, \tag{28}$$

where c denotes the unit computational complexity for a complex multiplication. $N_{c,i}$ represents the average number of complex multiplications for the ith step detection, where i=1,2.

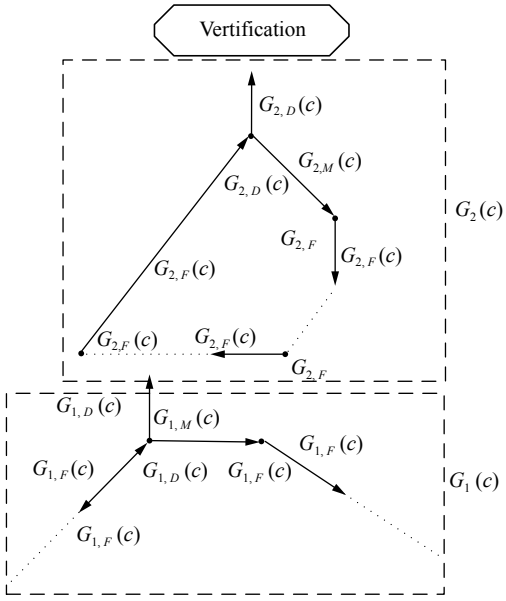

Fig. 3 Search state diagram of the TCAM

MAC [12] is the mean complex multiplications cost to detect correct parameters in GNSS acquisition. The theoretical MAC of the search state of TCAM in unit of c can be found as

$$\mu_c = \frac{\mathrm{d}G(c)}{\mathrm{d}c}|_{c=1} = \frac{\mathrm{d}G_1(c)}{\mathrm{d}c}|_{c=1} G_2(1) + \frac{\mathrm{d}G_2(c)}{\mathrm{d}c}|_{c=1} G_1(1) = \left[\frac{N_{c,1}}{P_{1,D}} + N_{c,1}(M_1 - 1)\left(\frac{1}{P_{1,D}} - \frac{1}{2}\right)\right]G_2(1) + \left[\frac{N_{c,2}}{P_{2,D}} + N_{c,2}(M_2 - 1)\left(\frac{1}{P_{2,D}} - \frac{1}{2}\right)\right]G_1(1). \tag{29}$$

When the detection probability is high ($P_{i,D} = 1$) and the false alarm probability is low ($P_{i,FA} = 0$), $G_1(1) = G_2(1) = 1$, and the lower bound of theoretical MAC of the search state can be written as

$$\mu_{cL} = 0.5\sum_{i=1}^{2}(M_i + 1)N_{c,i}. \tag{30}$$

Based on the analysis in [12], one complex multiplication is equal to two real multiplications, and based on Fig. 1, the average number of complex multiplications $N_{c,i}$ can be written as

$$N_{c,1} = N_B\frac{2K_\alpha + 1}{M_1}(N_s - N_B) + N_B\frac{M_1 - (2K_\alpha + 1)}{M_1}0.5(N_s - N_B), \tag{31}$$

$$N_{c,2} = \frac{2K_f + 1}{M_2}N_s + \frac{0.5}{M_2}\sum_{h_2}2^{h_2+1}. \tag{32}$$

To compare with TCAM, the FFT-based method, BASIC [21], is chosen as the compared method. The process of BASIC is shown in Fig 4.

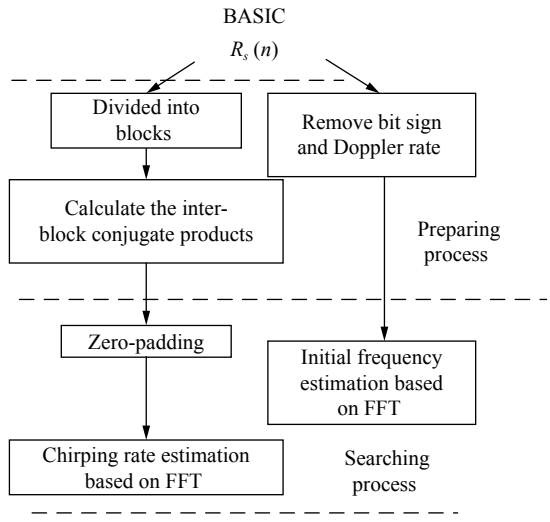

Fig. 4 Compared method BASIC

In the preparing process of BASIC, the number of complex multiplications about calculating the inter-block conjugate products is $N_B^2 \cdot \left(\frac{N_s}{N_B} - 1\right)$. When the bit sign and the Doppler rate are obtained, the number of complex multiplications about removing the Doppler rate is N_s. In the searching process of BASIC, due to the zero-padding process, the number of complex multiplications about Doppler rate estimation based on FFT per block is $M_1\log_2 M_1$. Thus the total number of complex multiplications about Doppler rate estimation based on FFT is $N_B \cdot \left(\frac{N_s}{N_B} - 1\right)(M_1\log_2 M_1)$. The number of complex multi-

plications about Doppler frequency estimation based on FFT is $M_2\log_2 M_2$. This is based on assumption [21] that the Doppler frequency range is [−250, 250] Hz, and [−500, 500] Hz/s.

In the preparing process of TCAM same as BASIC, the number of complex multiplications about calculating the differential signal and removing the Doppler rate is $N_B^2\cdot\left(\frac{N_s}{N_B}-1\right)+N_s$. Based on the analysis [12], (10) and (11) can be effectively performed by using only complex additions or complex subtractions, and the lower bound of MAC μ_{cL} is chosen as the number of complex multiplications in the searching process.

Based on the analysis above, the FFT based method BASIC needs to search all possible frequency parameters points by using complex multiplications. However, TCAM only needs to search a few possible frequency parameters points using complex multiplications, and search some possible frequency parameters points using real multiplications based on the set threshold. This is why the computational cost of TCAM is lower than that of BASIC. The total number of complex multiplications of methods can be shown in Table 1.

Table 1 Theoretical MAC comparison

Process	DCFT [29]	BASIC [21]	TCAM
Preparing process multiplication	$N_B\left(\frac{N_s}{N_B}-1\right)\cdot M_1\left(\frac{M_2}{\log_2 M_2}\right)$	$N_B^2\left(\frac{N_s}{N_B}-1\right)+N_s$	$N_B^2\left(\frac{N_s}{N_B}-1\right)+N_s$
Search process multiplication		$N_B\left(\frac{N_s}{N_B}-1\right)\cdot(M_1\log_2 M_1)+M_2\log_2 M_2$	μ_{cL}

In Table 1, $M_2=\lceil 2f_{dm}/\Delta_f+1\rceil$, and $M_1=\lceil 2\alpha_{0m}/\Delta_\alpha+1\rceil$, where α_0=$[-\alpha_{0m},\alpha_{0m}]$ Hz/s. The DCFT method needs two-dimensional FFTs which cost $M_2(M_1\log_2 M_1)$ complex multiplications. Moreover, there are N_s/N_B-1 blocks and n positions bit flipping. Every block needs the two-dimensional FFTs. Above all, the method DCFT costs $N_B(N_s/N_B-1)M_2(M_1\log_2 M_1)$ complex multiplications.

Based on Table 1, the theoretical MAC that equals to search process multiplications added by preparing process multiplications can be drawn as Fig. 5.

The Doppler rate range is assumed to be from −500 Hz/s to 500 Hz/s, and α_{0m}=500 Hz/s. Doppler frequency accuracy Δ_f is about $1/(2T)$ Hz, where T represents integration time or post-correlation signal length. Doppler rate accuracy Δ_α is set to be $1/(8M_\alpha N_s N_B T_s^2)$ Hz/s, where M_α=2. The Doppler frequency range is from −250 Hz to 250 Hz, and f_{dm}=250 Hz. The signal length ranges from 40 ms to 1 000 ms for integration.

It can be seen from Fig. 5 that the theoretical total number of complex multiplications increases when the signal length increases. Moreover, since (12), (17), and (18) are adopted, the computational cost of TCAM is much lower than that of the FFT based methods (BASIC and DCFT) under the same signal length.

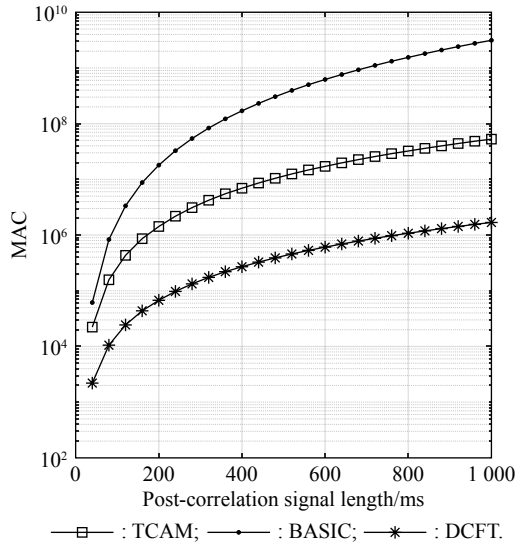

Fig. 5 MAC comparison

5. Detection performance comparison

To prove that TCAM has a low computational complexity, this section has been conducted by Matlab simulation and semi-physical simulation, and the FFT-based method BASIC has been chosen as a compared method with the simulated MAC as the computational criterion. The simulated parameters can be written as Table 2.

Table 2 Simulation parameters

Parameter	Value
Bit sign period N_B	20
Doppler frequency search range/Hz	[−250, 250]
Doppler rate search range/(Hz/s)	[−500, 500]
False alarm probability $P_{i,FA}$	0.002
Sampling time T_s/ms	1
Doppler frequency estimation resolution/Hz	$1/(2T)$
Doppler frequency estimation resolution	$1/\left(8M_\alpha N_s N_B T_s^2\right)$
Channel	AWGN channel
Number of Monte Carlo simulations	10 000

5.1 Performance comparison by Matlab

In this section, the MACs and detection probabilities of TCAM and BASIC have been simulated by Monte-Carlo simulation when frequency parameters (Doppler frequency and Doppler rate) and data bits change uniformly

in the range at each simulation.

In Fig 6. (a), since the approximation that $\left|\varphi_{b_0}\left(n_d,k_\alpha+\frac{g_1}{2^{h_1-1}}\right)\right|\approx\left|\varphi_{b_0}\left(n_d,k_\alpha+\frac{g_1+1}{2^{h_1-1}}\right)\right|$ in (12) and $\left|\varphi_2\left(n,k_f+\frac{g_2}{2^{h_2-1}}\right)\right|\approx\left|\varphi_2\left(n,k_f+\frac{g_2+1}{2^{h_2-1}}\right)\right|$ in (15) is adopted, the detection probability of TCAM is lower than that of BASIC. However, since the compressed processes based on (12), (15) and (17) with the detection based on the threshold is adopted, TCAM does not need to search all possible frequency parameter units, and many complex multiplications can be reduced. Thus in Fig 6. (b), the simulated MAC of TCAM is much lower than MACs of BASIC and DCFT at the same SNR condition.

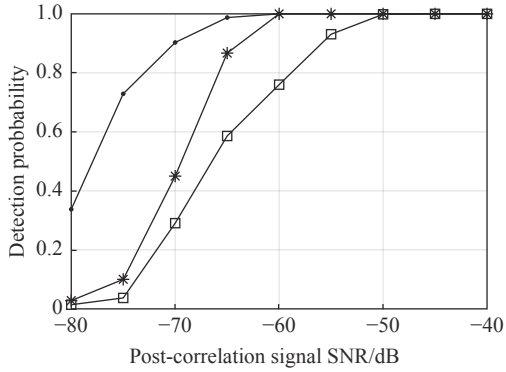

(a) Detection probabilities of Doppler rate and Doppler frequency

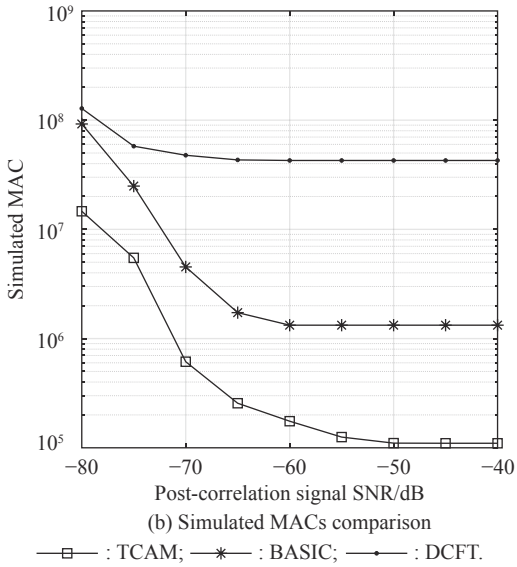

(b) Simulated MACs comparison

Fig. 6 Performance comparison in simulation

5.2 Performance comparison by semi-physical simulation

The post-correlation signal should be prepared for TCAM and BASIC (see Fig. 7). Firstly, the global position system (GPS) L1 C/A signal is produced by the signal simulator (HWA-RNSS-7200) and sent by its antenna. Then, the GPS intermediate frequency (IF) sampled data (IF is 4.092 MHz, the sampling frequency is 16.368 MHz, and the data type is int8) can be obtained by the IF signal collector. Finally, the post-correlation signal can be obtained based on (1) to (3). Then, based on configuration parameters of the simulator, the code phase can be obtained, and signals are correlated with the local code, respectively. $R_s(n)$ corresponding to the correct Doppler unit can be found, where the range of residual Doppler frequency α_0 is [−250, 250] Hz, and the range of α_0 is [−500, 500] Hz. Some noise is added to the post-correlation signal $R_s(n)$ for calculating simulated MACs in different SNRs, the post-correlation signal length is 100 ms.

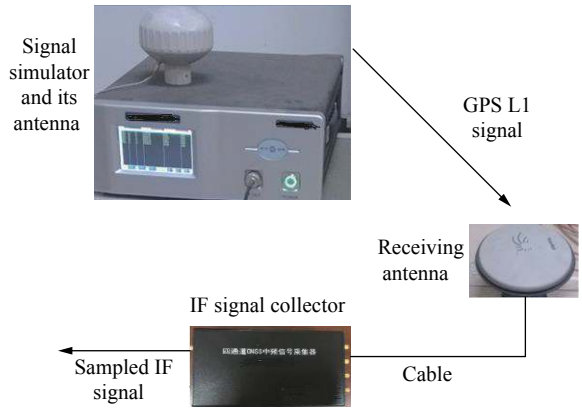

Fig. 7 Process to obtain IF signal of the GPS L1 C/A signal

In Fig. 8 (b), same as in Fig. 6 (b), it also proves that since compressed processes with the detection based on threshold is adopted, the simulated MAC of TCAM is much lower than MACs of BASIC and DCFT at the same SNR condition. When SNR is −40 dB, the TCAM's MAC in Fig. 8 (b) is lower than the TCAM's MAC in Fig. 6 (b). This is because MAC depends on set N_s based on (30) to (32). Moreover, N_s is set based on signal length. There are different signal lengths in the two figures.

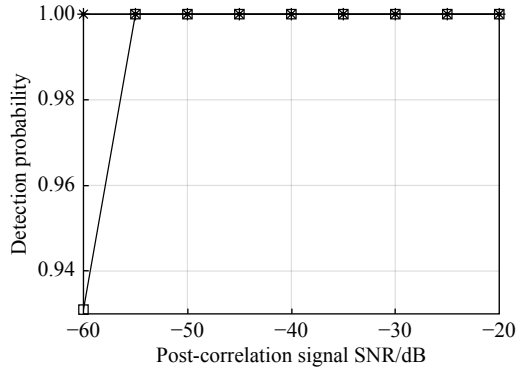

(a) Detection probabilities of Doppler rate and Doppler frequency

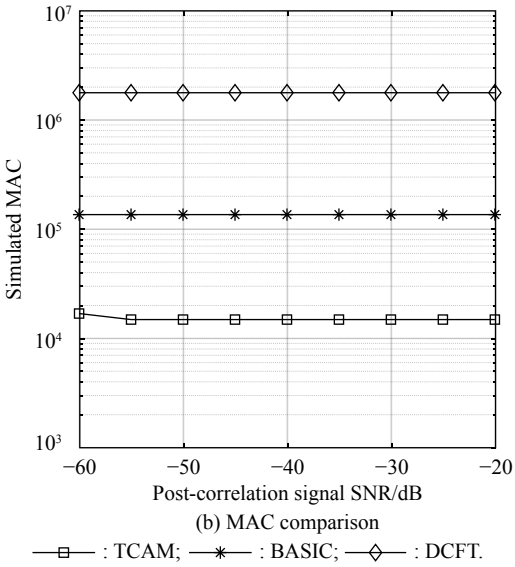

Fig. 8 Performance comparison in practical experiment

6. Conclusions

To further reduce the computational burden in high-dynamic and weak signal situations, we propose a two-step compressed acquisition method. Compression factors M_α and M_f are adopted in the set threshold detection. In this way, searching all possible frequency parameter units is not needed, and estimation accuracy can be improved based on (12), (15), and (17) with low computational complexity. The detection and false alarm probabilities of the proposed method are derived. Based on that, the theoretical MAC is derived. Moreover, in Fig. 5, the theoretical MAC of TCAM is much lower than MACs of BASIC and DCFT at the same post-correlation signal length. The test proves that although the detection probability of TCAM is lower than that of BASIC in Fig 6. (a), the simulated MAC of TCAM is much lower than the simulated MACs of BASIC and DCFT at the same SNR condition in Fig 6. (b) and Fig 8. (b).

References

[1] KONG S H. High sensitivity and fast acquisition signal processing techniques for GNSS receivers: from fundamentals to state-of-the-art GNSS acquisition technologies. IEEE Signal Processing Magazine, 2017, 34(5): 59–71.

[2] QAISAR S U, BENSON C R. Processing cost of Doppler search in GNSS signal acquisition: measuring Doppler shift in navigation satellite signals. IEEE Signal Processing Magazine, 2017, 34(5): 53–58.

[3] XIE F, SUN R, KANG G H, et al. A jamming tolerant BeiDou combined B1/B2 vector tracking algorithm for ultra-tightly coupled GNSS/INS systems. Aerospace Science and Technology, 2017, 70: 265–276.

[4] GAO F Q, XIA H X. Fast GNSS signal acquisition with Doppler frequency estimation algorithm. GPS Solutions, 2018, 22(4): 1–13.

[5] ZENG Q X, QIU W Q, ZHANG P N, et al. A fast acquisition algorithm based on division of GNSS signals. Journal of Navigation, 2018, 71(4): 933–954.

[6] JUAN B O, ROSA A V, FERNANDO G C. Energy efficient GNSS signal acquisition using singular value decomposition (SVD). Sensors, 2018, 18(5): 1586.

[7] WU C, GAO Y. Low-computation GNSS signal acquisition method based on a complex signal phase in the presence of sign transitions. IEEE Trans. on Aerospace and Electronic Systems, 2020, 56(6): 4177–4191.

[8] GUO W F, NIU X J, GUO C, et al. A new FFT acquisition scheme based on partial matched filter in GNSS receivers for harsh environments. Aerospace Science and Technology, 2016, 61: 66–72.

[9] KONG S H. A deterministic compressed GNSS acquisition technique. IEEE Trans. on Vehicular Technology, 2013, 62(2): 511–521.

[10] KONG S H, KIM B. Two-dimensional compressed correlator for fast PN code acquisition. IEEE Trans. on Wireless Communications, 2013, 12(11): 5859–5867.

[11] ZHU C, FAN X N. A novel method to extend coherent integration for weak GPS signal acquisition. IEEE Communications Letters, 2015, 19(8): 1343–1346.

[12] KONG S H. SDHT for fast detection of weak GNSS signals. IEEE Journal on Selected Areas in Communications, 2015, 33(11): 2366–2378.

[13] QIN F, ZHAN X Q, ZHAN L. Performance assessment of a low-cost inertial measurement unit based ultra-tight global navigation satellite system/inertial navigation system integration for high dynamic applications. IET Radar, Sonar & Navigation, 2014, 8(7): 828–836.

[14] ZHAN X Q, QIN F, DU G. Improvement of global navigation satellite system signal acquisition using different grade inertial measurement units for high dynamic applications. IET Radar, Sonar & Navigation, 2014, 8(3): 233–241.

[15] MA G J, YU B G, JIA R C, et al. INS-aided high dynamic GNSS rapid acquisition and stable tracking. Radio Engineering, 2016, 46(2): 23–26. (in Chinese)

[16] DUAN R F, LIU R K, ZHOU Y, et al. A carrier acquisition and tracking algorithm for high-dynamic weak signal. Lecture Notes in Electrical Engineering, 2013, 187: 211–219.

[17] GOMEZ-CASCO D, LOPEZ-SALCEDO J A, SECO-GRANADOS G. Optimal post-detection integration techniques for the reacquisition of weak GNSS signals. IEEE Trans. on Aerospace and Electronic Systems, 2020, 56(3): 2302–2311.

[18] ZHANG W, GHOGHO M. Computational efficiency improvement for unaided weak GPS signal acquisition. Journal of Navigation, 2012, 65(2): 363–375.

[19] LO PRESTI L, ZHU X, FANTINO M, et al. GNSS signal acquisition in the presence of sign transition. IEEE Journal of Selected Topics in Signal Processing, 2009, 3(4): 557–570.

[20] MA F H, GUO F C, YANG L. Direct position determination of moving sources based on delay and Doppler. IEEE Sensors Journal, 2020, 20(14): 7859–7869.

[21] YANG C, NGUYEN T, BLASCH E, et al. Post-correlation semi-coherent integration for high-dynamic and weak GPS signal acquisition. Proc. of the IEEE/ION Position, Location & Navigation Symposium, 2008: 1341−1349.

[22] YU W, ZHENG B, WATSON R, et al. Differential combining for acquiring weak GPS signals. Signal Processing, 2007, 87(5): 824–840.

[23] LI X S, GUO W. Efficient differential coherent accumula-

tion algorithm for weak GPS signal bit synchronization. IEEE Communications Letters, 2013, 17(5): 936–939.
[24] ESTEVES P, SAHMOUDI M, BOUCHERET M L. Sensitivity characterization of differential detectors for acquisition of weak GNSS signals. IEEE Trans. on Aerospace and Electronic Systems, 2016, 52(1): 20–37.
[25] WU C, XU L P, ZHANG H, et al. An improved acquisition method for GNSS in high dynamic environments: differential acquisition based on compressed sensing theory. Navigation, 2017, 64(1): 23–24.
[26] LUO Y R, ZHANG L, HANG R. An acquisition algorithm based on FRFT for weak GNSS signals in a dynamic environment. IEEE Communications Letters, 2018, 22(6): 1212–1215.
[27] FOUCRAS M, JULIEN O, MACABIAU C, et al. Probability of detection for GNSS signals with sign transitions. IEEE Trans. on Aerospace and Electronic Systems, 2016, 52(3): 1296–1308.
[28] FAN B, ZHANG K, QIN Y L, et al. Discrete chirp-Fourier transform-based acquisition algorithm for weak global positioning system L5 signals in high dynamic environments. IET Radar, Sonar & Navigation, 2013, 7(7): 736–746.
[29] WU C, XU L P, ZHANG H, et al. A block zero-padding method based on DCFT for L1 parameter estimations in weak signal and high dynamic environments. Frontiers of Information Technology & Electronic Engineering, 2015, 16(9): 796–804.
[30] LI H, CUI X W, LU M Q, et al. Dual-folding based rapid search method for long PN-code acquisition. IEEE Trans. on Wireless Communications, 2008, 7(12): 5286–5296.
[31] LI H, LU M Q, CUI X W, et al. Generalized zero-padding scheme for direct GPS P-code acquisition. IEEE Trans. on Wireless Communications, 2009, 8(6): 2866–2871.
[32] SIMON M K. Probability distributions involving Gaussian random variables. Springer US, 2006.

Biographies

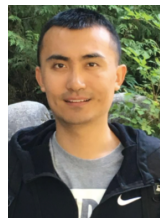

WU Chao was born in 1988. He obtained his Ph.D. degree from Xidian University, China in 2016. Now he works in Hangzhou Dianzi University. His research interests include GNSS signal acquisition and tracking.
E-mail: wuchao@126.com

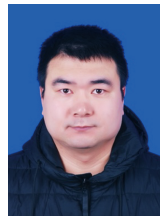

LIU Erxiao was born in 1984. He obtained his Ph.D. degree from Xidian University, China in 2013. Now he works in Hangzhou Dianzi University. His research interest is navigation signal processing.
E-mail: liuerxiao@hdu.edu.cn

JIAN Zhihua was born in 1978. He obtained his Ph.D. degree from Nanjing University of Posts and Telecommunications, China in 2008. Now he works in Hangzhou Dianzi University. His research interests include signal detection and tracking.
E-mail: jianzh@hdu.edu.cn